(Third Linz Workshop)

CONF-8308173--4

NOTICE

PORTIONS OF THIS REPORT ARE ILLEGIBLE. It has been reproduced from the best available copy to permit the broadest possible availability.

THE ROLES OF PAULI CORRELATIONS, CHANNEL COUPLINGS, AND SHAKE-OFF IN ION-INDUCED KL^V AND K^2L^V MULTIPLE-VACANCY PRODUCTION

Richard L. BECKER
Oak Ridge National Laboratory, Oak Ridge, TN 37831, USA

A. L. FORD and J. F. READING
Texas A & M University, College Station, TX 77843, USA

CONF-8308173--4

DE84 016564

Cross sections for target K-plus-L-shell multiple-vacancy production by ions can be inferred from experimental measurements of K x-ray and Auger satellite intensities. The theory of K^nL^v multiple-vacancy distributions has been generalized from the single-particle model (the statistically independent electron approximation) to the independent Fermi particle model. The Pauli correlations (electron exchange terms) are found to nearly cancel in many cases because of a tendency toward random phases. This results in the first quantal demonstration that the vacancy distribution is nearly binomial (but slightly narrower). Calculations have been generalized from the traditional first-order approximations to unitary approximations (first Magnus and coupled-channels) which correctly predict the saturation of the mean vacancy probability with increasing projectile charge. The recent availability of satellite and hypersatellite data for the same collision system makes possible the beginning of an investigation of the effects of increased removal energies and increased shaking in hypersatellites (K^2L^v) as compared with satellites. We review our unified treatment of ion-plus-shaking induced amplitudes for L-vacancy production accompanying ion-generated K-holes. Calculations for C^{6+} + Ne satellite and hypersatellite vacancy distributions are presented.

MASTER

By acceptance of this article, the publisher or recipient acknowledges the U.S. Government's right to retain a nonexclusive, royalty-free license in and to any copyright covering the article.

DISTRIBUTION OF THIS DOCUMENT IS UNLIMITED

EAB

1. Introduction

K-shell vacancy production by ion-impact remains a challenging problem in atomic theory because it occurs predominantly in close collisions, during which the interaction between the projectile and the target electrons becomes very strong. By contrast, inclusive L-shell vacancy production [1] is dominated by collisions with relatively large values of the impact parameter, several times the L-shell radius, for which the interaction is weak enough that the creation of a second L-shell vacancy or a K-hole occurs very infrequently. The close collisions can be distinguished experimentally by detecting the decay of a K-vacancy by measuring a K x-ray or a K Auger electron. Because of the strong Coulomb interaction in close collisions, the production of one or more L-holes in addition to the K-hole is quite probable. For light ions the relative probability KL^1/KL^0 is proportional to Z_p^2, where Z_p is the nuclear charge of the projectile. The energies of the K^1L^v hole configurations vary with the number of L-shell vacancies, v, as do the energies of the final states of the K_α decay process, K^0L^{v+1}, so that the decay energies depend on v. The configurations with one or more L-shell vacancies show up as satellites of the x-ray or Auger K_α diagram-line. Under moderate resolution one cannot distinguish experimentally among holes in the L_I, L_{II}, and L_{III} subshells ($2s_{1/2}$, $2p_{1/2}$, and $2p_{3/2}$ spin-orbitals). The probability of producing a second K-hole relative to a single K-hole is typically $\sim 10^{-4}$ in proton impact, but this relative probability also increases as Z_p^2 for small Z_p. The so-called hypersatellites, K^2L^v, have been measured in recent years with sufficient accuracy to provide good intensity distributions as a function of v. The KL^v and K^2L^v cross sections provide a wealth of data which presents a considerable challenge to the theory of atomic inner-shell collision physics.

The energies of the K satellites and hypersatellites are well understood in terms of the Hartree-Fock theory of hole configurations. The intensity distributions have been found empirically to obey to good approximation a binomial distribution. For a shell S with N spin-orbitals this distribution satisfies

$$1 = [\bar{p}_S + (1-\bar{p}_S)]^N = \sum_{v=0}^{n} P^{S^{N-v}}_{S^v} = \sum_{v=0}^{n} \binom{N}{v} (\bar{p}_S)^v (1-\bar{p}_S)^{N-v} \tag{1.1}$$

where the number-exclusive hyperinclusive (NEHI) probability [2] of precisely v vacancies and N-v occupancies in S is denoted by $P^{S^{N-v}}_{S^v}$, and the mean vacancy probability per electron is

$$\sum_{v=0}^{N} \frac{v}{N} P^{S^{N-v}}_{S^v} = \bar{p}_S. \tag{1.2}$$

This empirical observation is easily explained in terms of a semi-classical ("impact-parameter") treatment of the relative motion of the projectile and target, and a single-particle model (SPM) of the multiple-hole production. In this formulation the creations of the various holes are regarded as statistically independent, so that

$$P^{K^{2-n},L^{8-v}}_{K^n,L^v}(b) = P^{K^{2-n}}_{K^n}(b)\, P^{L^{8-v}}_{L^v}(b) \tag{1.3}$$

and each factor is given by eq. (1.1) with $p_S = p_K(b)$ or $p_L(b)$. Because $p_L(b)$ varies slowly for $0 \leq b \lesssim 4a_K$, where a_K is the Bohr radius of the K-shell, the SPM gives

$$\sigma^{K^{2-n},L^{8-v}}_{K^n,L^v} \cong \binom{8}{v} (\bar{p}_L)^v [1-\bar{p}_L]^{8-v}\, \sigma^{K^{2-n}}_{K^n}, \tag{1.4}$$

where

$$\sigma^{K^{2-n}}_{K^n} = 2\pi \binom{2}{n} \int_0^\infty db \cdot b\, p_K(b)^n [1-p_K(b)]^{2-n} \tag{1.5}$$

and $\overline{p}_L \cong p_L(0)$.

The binomial distribution is built into the SPM through the assumption that the holes are statistically independent, so that this model cannot account for any significant deviations from the binomial form such as the frequent occurrence of an experimental second moment which is smaller than that given by the binomial distribution. This remark holds even when one distinguishes the three L subshells with separate $\overline{p}_{L_I}$, $\overline{p}_{L_{II}}$, and $\overline{p}_{L_{III}}$. In the case of F^{9+} + Ne, a nearly symmetric collision system for which electron transfer to the projectile is highly probable at intermediate impact speeds, the observed satellite intensities deviate strongly from the binomial [3]. Thus, one challenge to collision theory is to provide a quantal many-electron theory which nearly reduces to the single-electron theory in many cases, but has the capability of providing somewhat narrower distributions and, in cases where one or two channels are dominant, can give strong deviations from the binomial. We have developed such a theory in the framework of the independent Fermi particle model (IFPM), which contains the effect of Pauli correlations. Their influence on the vacancy distribution will be discussed in § 2.

Because the binomial distribution is usually a fairly good approximation, emphasis can be centered on calculating $\overline{p}_L$, which nearly determines the L-shell distribution. All the calculations in the literature, aside from our work, have been limited to first-order collision approximations. These calculations have had enough success for proton and alpha impact to keep them in vogue for a decade, but they fail increasingly as Z_p is increased. This presents a severe gap in our understanding, because the most interesting cases are those with large $\overline{p}_L$. These are also the most important for applications of x-ray satellites to the study of electron densities in chemical compounds and solids [4].

The first-order approximations fail in several ways as Z_p increases: a) experimentally, the magnitude of $\bar{p}_L$ does not grow as Z_p^2, but saturates so as to remain < 1; b) a shift of the peak of the graph of $\bar{p}_L$ to higher impact speed is not predicted; and c) the width of this graph is not predicted to change with Z_p, whereas experimentally it broadens considerably. We have performed IFPM calculations both in the first Magnus approximation (a unitarized Born approximation) in which $\bar{p}_L$ is guaranteed to remain < 1 and also in the more refined coupled-channels approximation. Our results are discussed in § 3.

In K-shell photoionization, a first-order absorption process, for light targets a faint satellite line, K^1L^1, is seen. This is successfully understood as a K-shell photoionization together with a shake-off or shake-up of an L-shell electron resulting from the sudden change in the Hartree-Fock field when the K-electron is ejected [5]. For multiply-charged-ion impact $\bar{p}_L$, from below to quite a bit above its peak as a function of impact speed, is well described by direct multiple-electron excitation by the ion. However, for high speeds where $\bar{p}_L$ is well below its peak value, the "shaking" process must contribute significantly. Heretofore, this process has been included only as an additive, static contribution. We have noticed [6] that its contribution should be more than doubled for hypersatellites as compared to satellites. Also, we have realized that "shaking" is not a usual reaction mechanism in the sense of having a perturbing term in the Hamiltonian associated with it. We have developed a unified theory [6] of direct ionization and shaking in which the two "processes" interfere. This theory and an application to satellites and hypersatellites produced in C^{6+} + Ne collisions are discussed in § 4.

2. Pauli Correlations

In the IFPM the Pauli Exclusion Principle is satisfied so that the results of collision theory contain electron exchange terms, which imply statistical correlations among vacancies. Whereas the SPM leads trivially to the binomial distribution of multiple vacancies, the IFPM requires a very much more extensive analysis [7,2]. We shall only sketch the theoretical development and then discuss numerical results of calculations. First, we emphasize that we are dealing with inclusive processes [1,8] in which we must sum the cross sections of all reactions in which the specified conditions are met. For K^nL^v inclusive vacancy processes, we sum over the various holes which can be created in the M and higher shells and over the various multiplets contributing to a given K^nL^v configuration. Each <u>exclusive</u> reaction, $(h_1,\ldots,h_F) \to (k_1,\ldots,k_F)$ has a transition amplitude at impact-parameter b, given in terms of single-electron amplitudes, $a_{kh}(b)$, by

$$\langle k_1,\ldots k_N \mid A(b) \mid h_1,\ldots,h_N\rangle = \det[a_{kh}] \tag{2.1}$$

where k ranges over $k_1,\ldots,k_F$ and h over $h_1,\ldots,h_F$. The probability for this exclusive reaction is

$$\rho^{k_1,\ldots,k_F}(h_1,\ldots,h_F;b) = |\langle k_1,\ldots,k_F \mid A(b) \mid h_1,\ldots,h_F\rangle|^2. \tag{2.2}$$

Those <u>particular inclusive probabilities</u> for which only final vacancies are specified are defined for an F-electron system by

$$\rho_{\lambda_1,\ldots,\lambda_m}(F) \equiv \sum_{k_1<\ldots<k_F}{}' \rho^{k_1,\ldots,k_F}, \quad k_i \neq \lambda_i,\ldots,\lambda_m. \tag{2.3}$$

We find [8,2]

$$\rho_{\lambda_1,\ldots,\lambda_m}(F) = \det[\delta_{ij} - a^{(2)}_{\lambda_i,\lambda_j}], \quad i,j = 1,\ldots,m \tag{2.4}$$

where [7]

$$a^{(2)}_{k,k'}(b) \equiv \sum_{h}^{occ} a^{*}_{k,h}(b)a_{k',h}(b) = a^{(2)*}_{k',k}(b). \tag{2.5}$$

The SPM gives the approximation to (2.4), and to other related quantities, in which all the off-diagonal elements $a^{(2)}_{kk'}$ are dropped. These off-diagonal elements contain all the Pauli exchange terms. Next, we define hyperinclusive expected values [7,2] (which are not probabilities, but rather sums of them) for at least v vacancies in a set (a shell or sum of shells) S with N spin-orbitals, by

$$Q_{S^v} \equiv \sum'_{\lambda_1<\ldots<\lambda_v} \rho_{\lambda_1,\ldots,\lambda_v} < \binom{N}{v} \tag{2.6}$$

where each λ_i belongs to S. These can be expressed in terms of the NEHI probabilities by

$$Q_{S^v} = P_{S^v}^{S^{N-v}} + (v+1)P_{S^{v+1}}^{S^{N-v-1}} + \frac{(v+1)(v+2)}{1.2} P_{S^{v+2}}^{S^{N-v-2}} + \ldots . \tag{2.7}$$

The main result of the analysis is the inversion [7,2] of eq. (2.7) to give

$$P_{S^v}^{S^{N-v}} = Q_{S^v} - \binom{v+1}{1}Q_{S^{v+1}} + \binom{v+2}{2}Q_{S^{v+2}} + \ldots + (-)^{N-v}\binom{N}{N-v} Q_{S^N}. \tag{2.8}$$

The second term cancels that part of Q_{S^v} pertaining to v+1 vacancies; the third term cancels that part of the first two terms containing v+2 vacancies; etc. As a check of (2.8), we note that, if we neglect all the off-diagonal $a^{(2)}$'s and assume that all the diagonal $a^{(2)}$'s are the same,

$$\delta_{\lambda,\lambda'} - a^{(2)}_{\lambda,\lambda'}(b) \to p(b)\delta_{\lambda,\lambda'}, \quad \lambda,\lambda' \text{ in } S, \tag{2.9}$$

then

$$Q_{S^v}(b) \to \binom{N}{v} p(b)^v. \tag{2.10}$$

Equation (2.8) becomes

$$p^{S^{N-v}_{S^v}} + p^v \{\binom{N}{v} - \binom{v+1}{1}\binom{N}{v+1} p + \binom{v+2}{2}\binom{N}{v+2} p^2 + \ldots + (-)^{N-v}\binom{N}{N-v}p^{N-v}\} = \binom{N}{v}p^v(1-p)^{N-v}, \tag{2.11}$$

which is the SPM result, the binomial distribution. Equation (2.8) is readily computable; each Q is a small sum of low-order determinants. We refer to eq. (2.8) as the "vacancy formulation". There is an alternative "occupancy formulation" which involves hyperinclusive expected values, Q^{S^n}, for at least n final occupancies in the set S. An important check on the algebra is that numerical calculations with both formulations have always given the same results.

For application to the K^nL^v multiple vacancies, the formalism sketched above has been extended to NEHI probabilities in which the precise number of vacancies in each of two shells, K and L, is specified. Moreover, because the Coulomb interaction does not change the projection of intrinsic spin, we also separate the Q's into sums of products of spin-up and spin-down factors. The resulting expression for the satellite NEHI probabilities has been stated in ref. [1]. The results for the hypersatellites and for no K-hole are given, along with a full derivation, in ref. [2].

Let us examine some results of a coupled-channels calculation of C^{6+} + Ne collisions at 1 MeV/amu. The integrand of the double K-vacancy cross section, $\sigma^{K^0}_{K^2}$ of eq. (1.5), reaches its maximum near b = 0.41 a_K. The inclusive single-vacancy probabilities, ρ_h, are the same in both the SPM and the IFPM. Their values at b/a_K = 0.41 are ρ_{1s} = 0.014, ρ_{2s} = 0.573, ρ_{2p0} = 0.707, ρ_{2p+} = 0.436, and ρ_{2p-} = 0.418. Here 2p+ and 2p- are the symmetrical and antisymmetrical combinations, respectively, of the 2p orbitals with m = ±1. The average, L-shell,

inclusive, single-vacancy probability at this b value is $p_L^{SPM} = 0.535$. It applies both to satellites and hypersatellites. The first step in obtaining the effect of Pauli correlations is to evaluate the six off-diagonal elements of the density matrix $a^{(2)}$. In part A of table 1 we see that their magnitudes are considerably less than those of $(\rho_{h_1 h_2})^{1/2}$ and that their phases are well distributed [9] in the interval $(-\pi,\pi)$. The orbital $2p_-$ does not appear in the table because the only amplitude $a_{h,2p_-}$ which does not vanish because of invariance under time reversal is $a_{2p_-,2p_-}$, so that the only non-vanishing $a^{(2)}_{h,2p_-}$ is the diagonal element $a^{(2)}_{2p_-,2p_-} = 1-\rho_{2p_-}$. The $a^{(2)}$'s reduce the IFPM values of the particular inclusive multiple-vacancy probabilities, $\rho_{h_1 h_2 \cdots}$, below their SPM values, as shown in part B of table 1. The hyperinclusive expected values, eq. (2.6), are similarly reduced [1]. Equation (2.8) for the number-exclusive hyperinclusive (NEHI) probabilities $P^{K^{2-n},L^{8-v}}_{K^n,L^v}$ is an alternating series. The alternation of signs tends to further lessen the difference between the IFPM and SPM results for the NEHI probabilities. The resulting IFPM distribution for the hypersatellites, $P^{K^0,L^{8-v}}_{K^2,L^v}$ $(0.41\ a_K)$, is shown in the shaded histogram of fig. 1. The IFPM mean L-shell hypersatellite vacancy probability per electron, obtained from this distribution by eq. (1.2), is $p_L^{(2)} = 0.463$, which is 13.3% less than the SPM value. The binomial distribution with $p_L^{(2)} = 0.463$ is shown in the unshaded histogram of fig. 1. One sees that the IFPM distribution is close to the binomial distribution with the same value of $p_L^{(2)}$. We have used a logarithmic scale in fig. 1 in order to show that in the wings (v=0,1,7,8) the binomial values are more than a factor 2 times the IFPM values. The IFPM distribution is thus narrower and more sharply peaked than the corresponding binomial distribution. A measure of the width is the normalized variance $\langle(v - \langle v\rangle)^2\rangle/\langle v\rangle^2$, which is (1-p)/8p for a binomial distribution. The normalized variance of the

IFPM hypersatellite distribution at 0.41 a_K is only 0.102/0.145 ≈ 70% of that of the binomial distribution, and 75% of that of the "subshell binomial" distribution, with the same p_L value. For the IFPM satellite distribution, $p_L^{(1)}$ = 0.499; and for the "no K-vacancy" case, $p_L^{(0)}$ = 0.536. These are 6.6% lower and 0.24% greater, respectively, than the SPM value. The weighted average of the three IFPM values equals the SPM value, where the weight factors are $\binom{2}{n}(\rho_{1s})^n(1-\rho_{1s})^{2-n}$, n=0,1,2.

After integration over the impact parameter, we obtain in the IFPM(SPM) $\bar{p}_L^{(2)}$ = 0.451(0.530), $\bar{p}_L^{(1)}$ = 0.450(0.489), and $\bar{p}_L^{(0)} = 0.159^{-2}$ (0.159^{-2}). The "no K-vacancy" cross section is dominated by large b-values where $p^{(0)}(b)$ is small so that hole-hole correlations are negligible. The weight factor for the double K-vacancies is concentrated at smaller b-values than that for the satellites. Hence the SPM ratio $\bar{p}_L^{(2)}/\bar{p}_L^{(1)}$ is 8% greater than one. However, in the IFPM at each b $p^{(2)}(b)/p^{(1)}(b)$ is less than one so that $\bar{p}_L^{(2)}/\bar{p}^{(1)}$ is only 0.2% greater than one. We return to the comparison between hypersatellite and satellite $\bar{p}_L$ values in § 4, where we include shaking contributions and also take into account (crudely) the fact that the removal energies for hypersatellites are greater than those for satellites. These two effects operate in opposite directions.

3. Saturation of $\bar{p}_L(Z_p)$ in coupled-channels collision theory

The most glaring failure of first-order collision approximations, whether wave-mechanical Born, semi-classical Born (SCA), or binary encounter impulse approximation (BEA) is that $\bar{p}_L$ grows too rapidly with Z_p and eventually exceeds unity. In the SPM

$$p_L(Z_p,b) \equiv \sum_p^{\text{unocc}} \langle | a_{\lambda,p}(Z_p,b) |^2 \rangle_L = Z_p^{\,2}\, p_L(1,b) \qquad (3.1)$$

where the sum is over all initially unoccupied spin-orbitals and the average is over all the spin-orbitals λ in the L-shell. Equation (3.1) is an immediate consequence of the fact that the off-diagonal, first-order, collision amplitudes are proportional to Z_p.

In order to keep $p_L(Z_p) < 1$, it is essential to use a unitary collision approximation, i.e. one in which probability is conserved. One of the simplest of these is the first Magnus (M1) approximation [10]. If the time-development matrix in first-order theory, $U^{(1)}(t,t')$, has the asymptotic limit

$$U^{(1)}_{j,k}(\infty,-\infty) = a^{(1)}_{j,k} = \delta_{j,k} - i[\hat{B}^{(1)}]_{j,k}, \tag{3.2}$$

the corresponding matrix for the M1 approximation is

$$a^{(M1)}_{j,k} = [\exp(-i\,\hat{B}^{(1)}]_{j,k}. \tag{3.3}$$

Here, with the Hamiltonian $H = H_0+V(t)$, in the interaction picture,

$$\hat{B}^{(1)} = \int_{-\infty}^{\infty} dt'\, e^{iH_0t'}\, V(t')e^{-iH_0t'}. \tag{3.4}$$

$\hat{B}^{(1)}$ is Hermitian, so that $a^{(M1)}$ is unitary.

Figure 2 shows results of M1 calculations in the IFPM of $\overline{p}_L/Z_p{}^2$ versus impact energy per nucleon for H^+, He^{2+}, C^{6+}, and F^{9+} ions on atomic argon. By contrast, for SCA calculations in the SPM, the curves for all values of Z_p would be coincident and would lie very near the first Magnus curve for protons. The peak value, $(\overline{p}_L/Z_p{}^2)_{max} \approx 0.024$, would then imply for F^{9+} that $(\overline{p}_L)^{SCA}_{max} \approx 2$. The M1 peak value for F^{9+}, on the other hand, is only about 0.4.

Although the M1 approximation gives saturation of $\overline{p}_L$ with Z_p, we can obtain greater accuracy by doing coupled-channels calculations. For the M1 and the coupled-channels calculations we employed a large set of target-centered spin-orbitals calculated by diagonalizing the Hartree-Fock Hamiltonian of the argon

ground state in an underlying basis of normalized, complex, exponential functions. The resulting pseudostates consist of very good approximations to the occupied Hartree-Fock states together with localized spin-orbitals with pseudoenergies greater than zero. The latter have been found to give a good description of ionization. The basis contained nine radial functions for each value of angular momentum ℓ, where ℓ = 0, 1, 2, and 3. In the coupled-channels calculations all the pseudostates were allowed to mix during each of very many time steps, Δt. The resulting curves [4] for $\bar{p}_L/Z_p^2$ also are shown in fig. 2. One sees that the deviations of the coupled-channels curves from the M1 curves increase with Z_p. A comparison of the coupled-channels curves with the available experimental data is given in ref. [4]. We note that the theory predicts that as Z_p increases, the peak value moves to higher impact speed and the peak broadens. These features are in agreement with experiment.

The absolute magnitude of the calculated $\bar{p}_L$ is very good for protons, but becomes steadily worse as Z_p increases. For Z_p = 9, $\bar{p}_L$ is overestimated by up to a factor of 1.7. We attribute the overestimate to a failure of the IPM to employ large enough removal energies for multiple-vacancy production. In the IPM the removal energy for m holes i=1,2,..,m is

$$E^{(m)} = \sum_{i=1}^{m} \varepsilon_i$$

where ε_i is the Hartree-Fock energy eigenvalue for spin-orbital i. These eigenvalues are good approximations to the corresponding first ionization potentials, $I_i^{(1)}$. If we think of the holes as created in succession beginning with the least bound, the correct removal energy is

$$R^{(m)} = I_1^{(1)} + I_2^{(2)} + \ldots + I_m^{(m)}$$

where $I_i^{(i)}$ is the i^{th} ionization potential, namely, that for spin-orbital i in the Hartree-Fock potential in which i-1 higher lying electrons have already been removed. Our partially successful efforts to overcome this difficulty of the "non-additivity of first ionization potentials" is discussed in ref. [1] and also below in connection with figs. 3 and 4.

4. Unification of collision and shake contributions to K^2L^v hole production

For very light elements the relative change in the Hartree-Fock field produced by the removal of an inner electron is much greater than it is for heavy elements. Also the change resulting from the removal of two K-shell electrons is roughly twice that from the removal of only one. Thus, one may expect to see the effect of "shaking" most prominently in the hypersatellites of light elements. In the past, the primary collision event and shaking have been treated as successive events. In that approach one would calculate NEHI probabilities for multiple-vacancy production by ion-impact, $\overline{P}$, and then matrix multiply these probabilities by a shaking probability, P^{Sh}, to get final probabilities

$$P^{K^{2-n},L^{8-v}}_{K^n,L^v}(Z_p,E,b) = \sum_{v'} P^{Sh}_n(v,v')\overline{P}^{K^{2-n},L^{8-v'}}_{K^n,L^{v'}}(Z_p,E,b), \qquad n=1,2 \tag{4.1}$$

The shake-off plus shake-up probability matrix is independent of Z_p, the impact energy E, and the impact parameter.

In practice, the shaking process has been almost completely neglected for ion impact, although it has been examined carefully [5] for photon and electron impact ionization of the K-shell, for which the small $\overline{p}_L$ is produced almost entirely by shaking. For impact by multiply charged ions, the peak value of $\overline{p}_L(E)$ is so large that the shake contribution to it is negligible. Only for energies well above that of its peak does $\overline{p}_L$ become small enough for shaking to

show up. Nevertheless, this high-energy region is accessible experimentally, and comparison of $\bar{p}_L$'s for hypersatellites and satellites should yield information on shaking. Interpretation is complicated by the fact that for hypersatellites the L-shell removal energies are greater than for satellites. This tends to reduce $\bar{p}_L$, whereas the greater shaking tends to increase $\bar{p}_L$ for hypersatellites. So far there have been very few such pairs of data. R. L. Watson, O. Benka et al. [11] have obtained both $\bar{p}_L$ values in neon at E/A approximately equal to 1.35 MeV for Z_p = 2, 6, 12, and 18 (with mean ionic charges $\bar{q}$ of 1.8 ± 0.2, 5.1 ± 0.2, 8.6 ± 0.4, and 13.0 ± 0.5, respectively). The satellite and hypersatellite $\bar{p}_L$ values are nearly the same at this impact speed. However, for the smallest Z_p (He ions) the hypersatellite value (0.13) is 18% greater than the satellite value (0.11), which may possibly be showing the greater shaking for hypersatellites. Unfortunately, such data are not yet available as a function of velocity.

With the aim of stimulating more extensive measurements, we have developed a unified theory [6] of ion-impact and shaking contributions to vacancy production in the L-shell accompanying impact-induced single or double K-vacancy production. Because both processes lead to the same final states, a quantal treatment should deal with interfering amplitudes rather than only with probabilities. In first-order perturbation theory, two perturbing potentials V_1 and V_2 lead to transition amplitudes

$$a_{kh}^{(1)} = a_{kh}^{(1,1)} + a_{kh}^{(1,2)}$$

where $a^{(1,1)}$ is caused by V_1 and $a^{(1,2)}$ by V_2. In higher orders of perturbation theory there are terms which arise from both potentials. A familiar two-potential problem is that of combined nuclear and Coulomb forces for p-p scattering. In the present problem we circumvent the explicit introduction of the

change in the HF Hamiltonian by the removal of one or two K electrons, and make use only of the two sets of HF pseudoeigenfunctions. We make the ansatz that the impact-induced transition amplitudes, $a_{k,h}(b)$, are calculated with the initial pseudostates and that the physical transition amplitudes including shaking can be obtained simply by projecting the impact amplitudes onto the final ("shaken") basis, $\{\phi_k^f\}$. This sudden approximation gives the "unified" scattering amplitudes [6]

$$s_{k,h}(Z_p,E,b) \equiv \sum_{k'} \langle \phi_k^f \mid \phi_{k'} \rangle \, a_{k',h}(Z_p,E,b) \tag{4.2}$$

$$= a_{k,h}(Z_p,E,b) + \sum_{k'} \Omega^{(1)}_{k,k'} a_{k',h}(Z_p,E,b) \tag{4.3}$$

where we have let [1]

$$\langle \phi_k^f \mid \phi_{k'} \rangle = \delta_{k,k'} + \Omega^{(1)}_{k,k'} \tag{4.4}$$

Care must be taken to place a constraint on the relation between the initial and final bases in order to prevent "spontaneous" shaking in the absence of a collision [6]. The term in (4.3) containing the shaking factor $\Omega^{(1)}$ also involves the impact amplitudes $a_{k',h}$ and consequently depends on Z_p and E. Only at very high energies where (see (3.2))

$$a_{k,h} \to \delta_{k,h} - i\, B^{(1)}_{k,h}, \tag{4.5}$$

with $B^{(1)}$ small, do we get a dominant, static, pure shaking term, $\Omega^{(1)}_{k,h}$, in

$$s_{k,h} = \delta_{k,h} + \Omega^{(1)}_{k,h} - i \sum_{k'} \langle \phi_k^f \mid \phi_{k'} \rangle \, B^{(1)}_{k',h}. \tag{4.6}$$

The rate at which this asymptotically high energy limit is reached depends on Z_p. This can be seen by comparing fig. 4 below (C^{6+} + Ne hypersatellites) with fig. 2 of ref. 6 (He^{2+} + Ne hypersatellites).

We have performed first Magnus and coupled-channels calculations in the IFPM for C^{6+} + Ne for comparison with the satellite and hypersatellite $\overline{p}_L$ values of Watson, Benka, et al. [11]. Figure 3 shows the satellite and fig. 4 the hypersatellite results for impact energies between 1 and 10 MeV/amu. The long dashed curve and the long and short dashed curve above 2.5 MeV/amu are first Magnus results without and with shaking, respectively. The first Magnus approximation becomes inaccurate at lower energies, where we have done coupled-channels calculations (---O--) without shaking. The extrapolations of the coupled-channels curves would join the coresponding first Magnus curves at E/A = 3 to 4 MeV. The full square is the datum of ref. 11 plotted at the initial beam energy, E/A = 1.83 MeV [12]. It lies at about 3/4 the coupled-channels value, so we are not yet in a position to test the unified theory. The full-triangle satellite value is from Kauffman et al. [3] at 1.5 MeV/amu.

All of the above-mentioned curves were calculated with the initial basis of the HF ground state of Ne. The open triangles and squares represent first Magnus values obtained with the "final" $(1s)^{-1}$ and $(1s)^{-2}$ HF configurations, respectively. The full circles (and —— -- curves) are coupled-channels values from the $(1s)^{-2}$ HF configuration. Even these lie slightly above the experimental values. However, the initial conditions are not handled properly as yet in these calculations. We should first project the initial states onto the "final" $(1s)^{-1}$ or $(1s)^{-2}$ basis and then calculate the impact amplitudes. We obtain a formulation alternative to that of eq. (4.2),

$$s_{k,h} = \sum_{k'} a_{k,k'} \langle \phi^f_{k'} | \phi_h \rangle, \tag{4.7}$$

where here the intermediate states belong to the final basis. Calculations with this formulation are in progress. Many more data are needed at high energies.

Experiments with fully stripped projectiles would be especially valuable. Separation of the effects of non-IFPM removal energies and shaking remains an interesting, fundamental problem.

This research was sponsored at ORNL by the U.S. Department of Energy, Division of Basic Energy Sciences under Contract No. W-7405-eng-26 with Union Carbide Corporation and at Texas A & M University by the NSF under Grant No. PHY-7909146 and the Center for Energy and Mineral Resources.

DISCLAIMER

This report was prepared as an account of work sponsored by an agency of the United States Government. Neither the United States Government nor any agency thereof, nor any of their employees, makes any warranty, express or implied, or assumes any legal liability or responsibility for the accuracy, completeness, or usefulness of any information, apparatus, product, or process disclosed, or represents that its use would not infringe privately owned rights. Reference herein to any specific commercial product, process, or service by trade name, trademark, manufacturer, or otherwise does not necessarily constitute or imply its endorsement, recommendation, or favoring by the United States Government or any agency thereof. The views and opinions of authors expressed herein do not necessarily state or reflect those of the United States Government or any agency thereof.

Table 1

Effect of Pauli correlations in coupled-channels calculations for C^{6+} + Ne at E/A = 1.0 MeV/amu and b = 0.41 a_K employing the HF potential [13] of the $(1s)^{-1}$ configuration of Ne. The various vacancies must have the same projection of intrinsic spin.

A. Off-diagonal, single-electron, transition-density matrix elements: normalized magnitude, $M^{(2)}_{h_1h_2} \equiv |a^{(2)}_{h_1h_2}| / (\rho_{h_1}\rho_{h_2})^{1/2}$, and phase.

h_1	h_2	$M^{(2)}_{h_1h_2}$	$ph(a^{(2)}_{h_1h_2})$
1s	2s	0.5786	-112.5°
	$2p_0$	0.3582	22.1°
	$2p_+$	0.0690	- 87.7°
2s	$2p_0$	0.3955	93.2°
	$2p_+$	0.0591	177.8°
$2p_0$	$2p_+$	0.0657	58.3°

B. Inclusive particular multiple-vacancy probabilities, $\rho_{h_1,h_2,\ldots}$.

h_1	h_2	h_3	h_4	ρ^{IFPM}	ρ^{SPM}	ρ^{IFPM}/ρ^{SPM}
1s	2s			5.44^{-3}	8.17^{-3}	0.666
1s	$2p_0$			8.79^{-3}	1.01^{-2}	0.870
1s	$2p_+$			6.19^{-3}	6.22^{-3}	0.995
2s	$2p_0$			3.42^{-1}	4.05^{-1}	0.844
2s	$2p_+$			2.49^{-1}	2.50^{-1}	0.996
$2p_0$	$2p_+$			2.44^{-1}	2.45^{-1}	0.996
1s	2s	$2p_0$		1.492^{-3}	5.780^{-3}	0.258
1s	2s	$2p_+$		2.187^{-3}	3.566^{-3}	0.613
1s	$2p_0$	$2p_+$		3.801^{-3}	4.399^{-3}	0.864
2s	$2p_0$	$2p_+$		1.473^{-1}	1.768^{-1}	0.833
1s	2s	$2p_0$	$2p_+$	7.040^{-4}	2.521^{-3}	0.279

References

[1] R. L. Becker, A. L. Ford, and J. F. Reading, Nucl. Instr. and Meth. 214 (1983) 49.

[2] R. L. Becker, A. L. Ford, and J. F. Reading, "Multiple Vacancy Production in the Independent Fermi Particle Model," submitted to Phys. Rev. A.

[3] R. L. Kauffman, C. W. Woods, K. A. Jamison, and P. Richard, Phys. Rev. A11 (1975) 872.

[4] R. L. Becker, A. L. Ford, and J. F. Reading, in Proc. 3rd Intern. Conf. on Particle Induced X-ray Emission (Heidelberg, July, 1983), to be published. (See also experimental papers by S. Raman, R. Vane, et al., loc. cit.)

[5] A very recent paper on shake theory, from which the literature can be traced, is K. G. Dyall, J. Phys. B: At. Mol. Phys. 16 (1983) 3137.

[6] R. L. Becker, A. L. Ford, and J. F. Reading, IEEE Trans. Nucl. Sci. NS-30 (1983) 1076.

[7] R. L. Becker, J. F. Reading, and A. L. Ford, IEEE Trans. Nucl. Sci. NS-28 (1981) 1092.

[8] J. F. Reading, Phys. Rev. A8 (1973) 3262; J. F. Reading and A. L. Ford, Phys. Rev. A21 (1980) 124; J. Reinhardt, B. Müller, W. Greiner, and G. Soff, Phys. Rev. Lett. 43 (1979) 1307.

[9] R. L. Becker, A. L. Ford, and J. F. Reading, Bull. Am. Phys. Soc. 26 (1981) 1309 and p. 136 in Intern. Conf. X-Ray and Atomic Inner-Shell Phys., Program and Abstracts, vol. 1, ed. by B. Crasemann (Physics Dept., Univ. Oregon, Eugene, 1982).

[10] W. Magnus, Comm. Pure Appl. Math. 7 (1954) 649; P. Pechukas and J. C. Light, J. Chem. Phys. 44 (1966) 3897.

[11] R. L. Watson, O. Benka, K. Parthasaradhi, R. J. Maurer, and J. M. Sanders,

J. Phys. B: At. Mol. Phys. 16 (1983) 835.

[12] Corrected for energy loss in the entrace window and in the Ne gas, the average C^{2+} beam energy is quoted as 1.4 MeV/A.

[13] P. S. Bagus, Phys. Rev. 139 (1965) A619.

Figure Captions

Fig. 1. Histogram of the L-shell, multiple-vacancy probability distribution for hypersatellites (double K-vacancies) produced in C^{6+} + Ne collisions at 1.0 MeV/amu and b = 0.4085 a_K as given by coupled-channels calculations in a large target-centered atomic basis. IFPM and binomial results are shaded and unshaded, respectively; both have $p_L^{(2)} = 0.46257$.

Fig. 2. Scaled mean L-shell vacancy probability per electron, $\bar{p}_L/Z_p^2$, versus impact energy per nucleon for satellites (single K-shell vacancy) in argon produced by ions with nuclear charges Z_p = 1, 2, 6, and 9, as given by first Magnus and coupled-channels calculations.

Fig. 3. Satellite $\bar{p}_L$ for C^{6+} + Ne collisions as a function of impact energy per nucleon. The two experimental data (▲ and ■) and the first Magnus and coupled-channels curves and points are described in the text.

Fig. 4. Hypersatellite $\bar{p}_L$ versus projectile energy per atomic mass unit for C^{6+} + Ne collisions. The experimental datum (▣) is from ref. 11. The first Magnus curves with and without shakeoff, the first Magnus points calculated without shakeoff in the $(1s)^{-1}$ (Δ) and $(1s)^{-2}$ (□) HF potential, and the coupled-channels curves without shakeoff calculated in the HF ground state (0) and $(1s)^{-2}$ (•) configurations are discussed in the text.

ORNL-DWG 83-18257

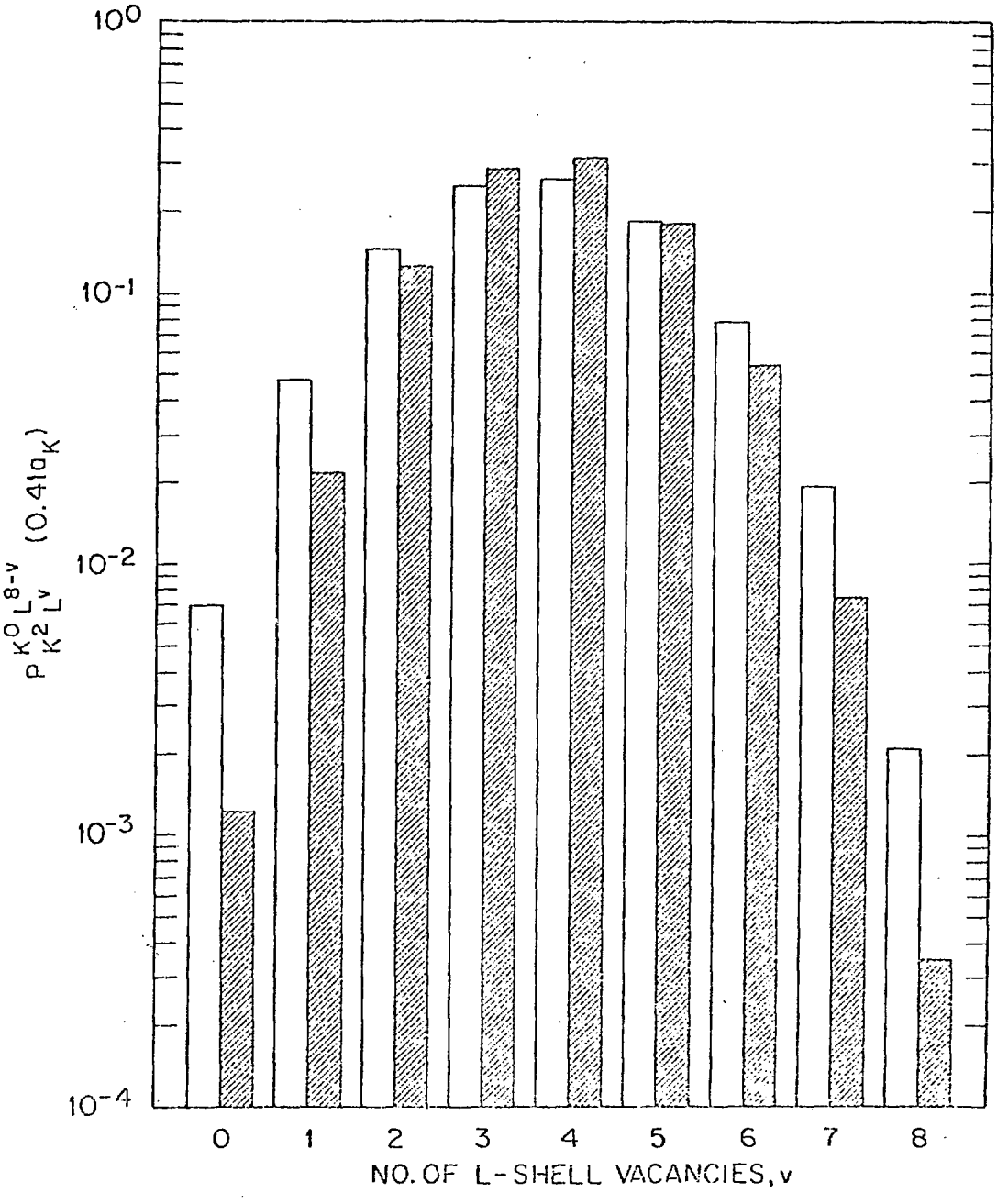

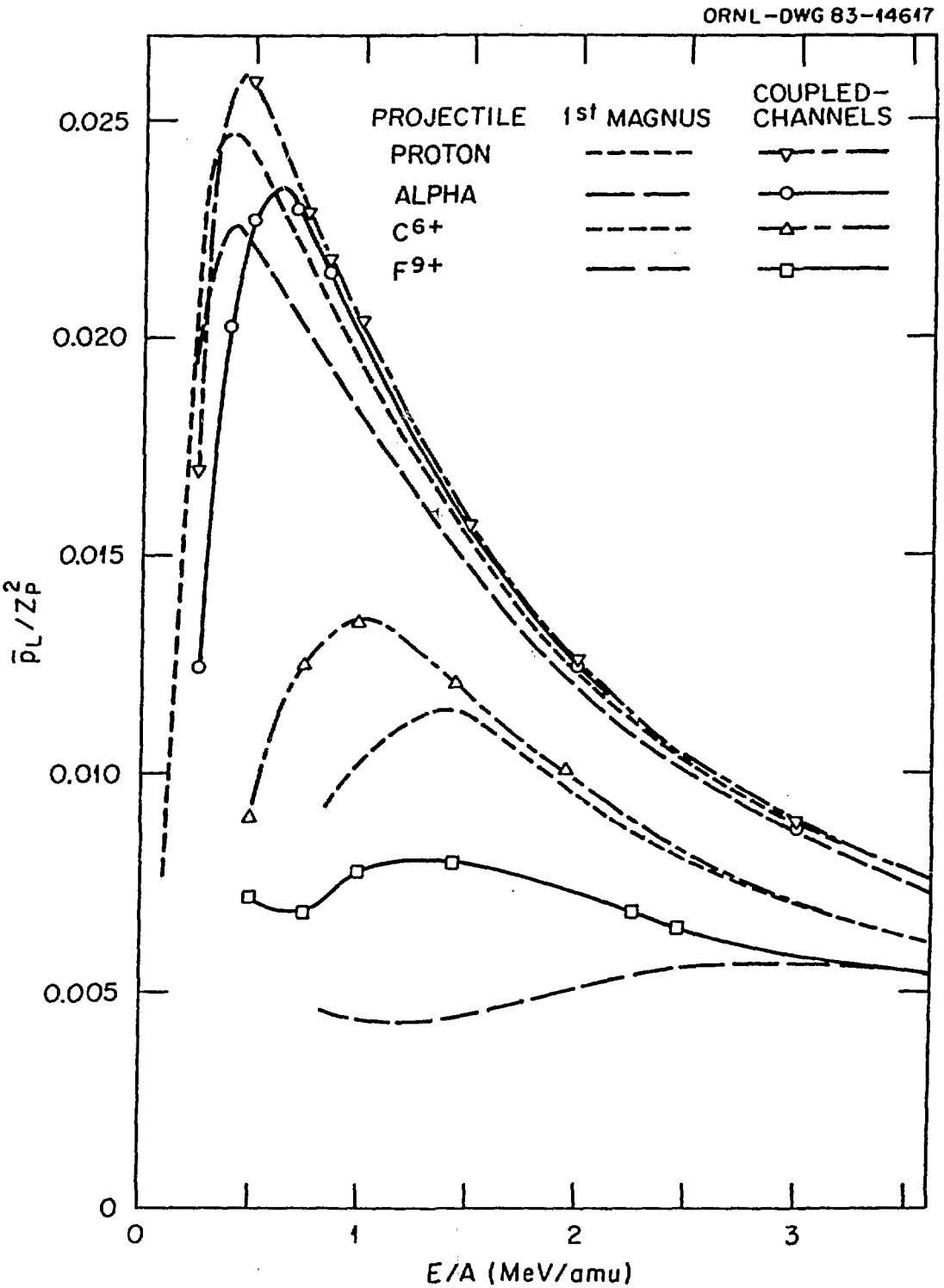
ORNL-DWG 83-14617
PROJECTILE
1st MAGNUS
COUPLED-CHANNELS
PROTON
ALPHA
C6+
F9+
0.025
0.020
0.015
0.010
0.005
0
0
1
2
3
E/A (MeV/amu)
$\bar{\rho}_L / Z_P^2$

Fig. 2

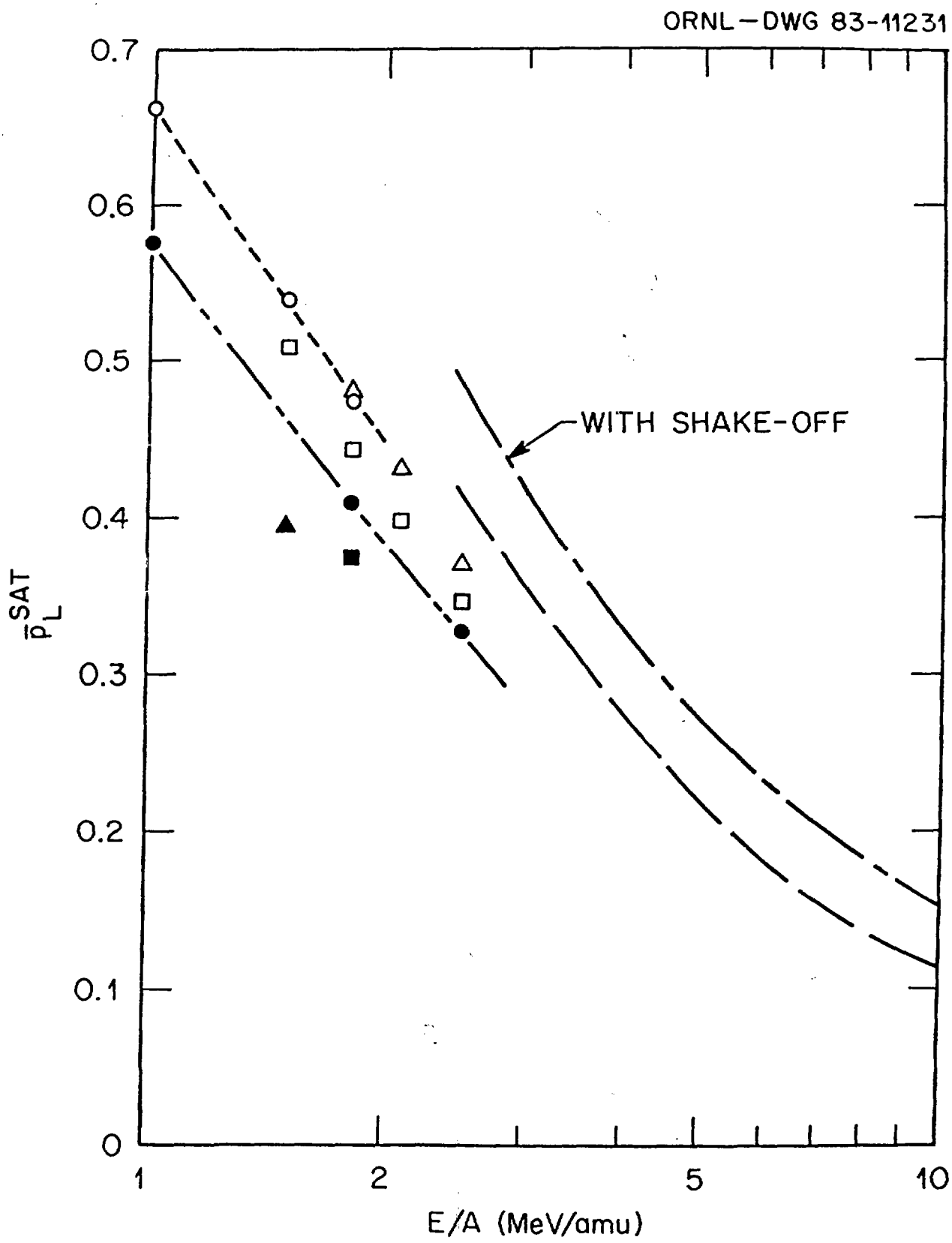
ORNL—DWG 83-11231
0.7
0.6
0.5
0.4
0.3
0.2
0.1
0
$\bar{p}_L^{SAT}$
WITH SHAKE-OFF
1
2
5
10
E/A (MeV/amu)

Fig. 3

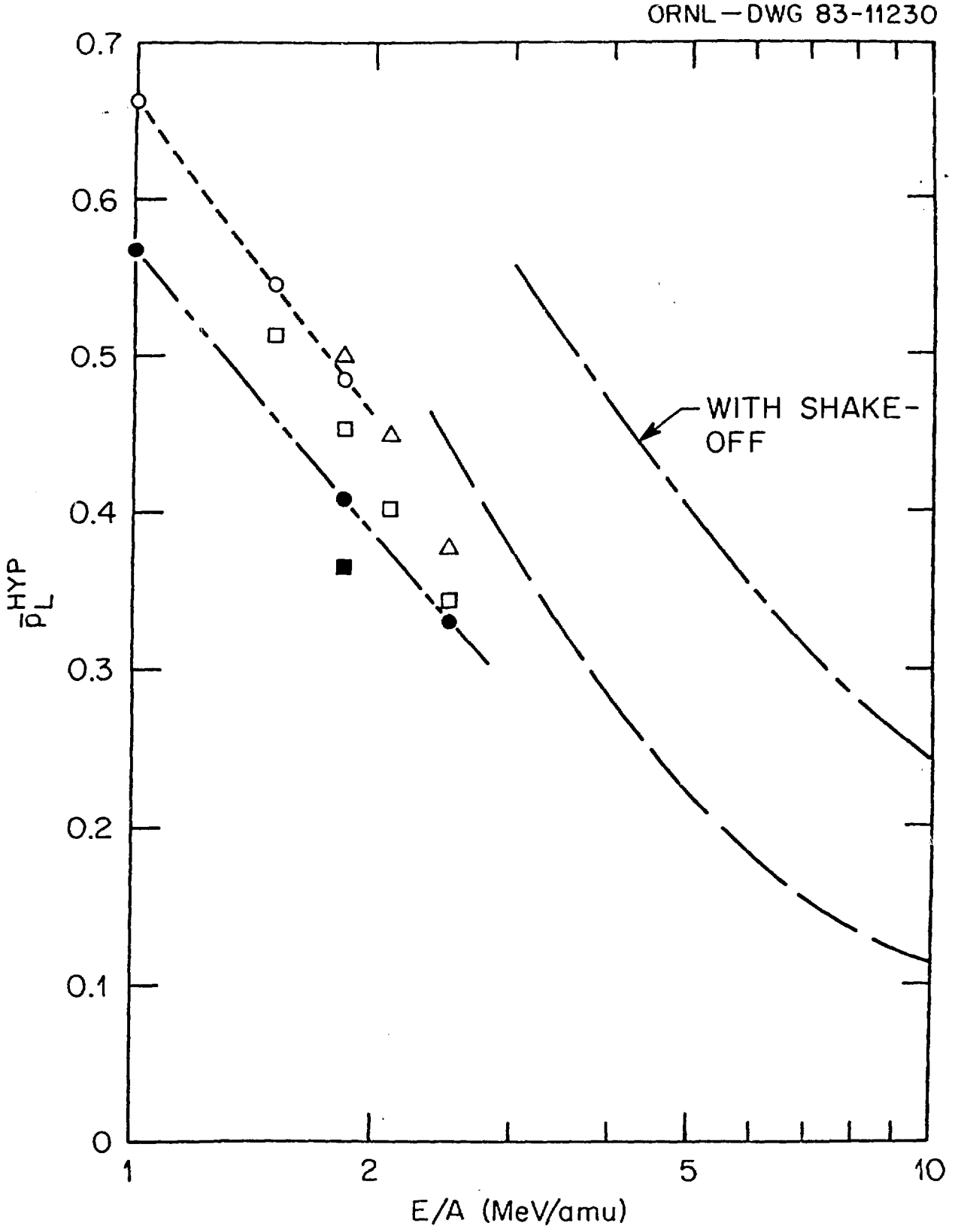
ORNL—DWG 83-11230
0.7
0.6
0.5
0.4
0.3
0.2
0.1
0
$\bar{p}_L^{HYP}$
WITH SHAKE-OFF
1
2
5
10
E/A (MeV/amu)

Fig. 4